Dissecting Homo-Heptamer Thermodynamics by Isothermal Titration Calorimetry: Entropy-Driven Assembly of Co-Chaperonin Protein 10

Kathryn Luke,* David Apiyo,* and Pernilla Wittung-Stafshede*†‡
*Department of Biochemistry and Cell Biology, †Keck Center for Structural Computational Biology, and ‡Department of Chemistry, Rice University, Houston, Texas

ABSTRACT Normally, isothermal titration calorimetry (ITC) is used to study binding reactions between two different biomolecules. Self-association processes leading to homo-oligomeric complexes have usually not been studied by ITC; instead, methods such as spectroscopy and analytical ultracentrifugation, which only provide affinity and Gibbs-free energy (i.e., K_D and ΔG), are employed. We here demonstrate that complete thermodynamic descriptions (i.e., K_D, ΔG, ΔH, and ΔS) for self-associating systems can be obtained by ITC-dilution experiments upon proper analysis. We use this approach to probe the dissociation (and thus association) equilibrium for the heptameric co-chaperonin proteins 10 (cpn10) from *Aquifex aeolicus* (*Aa*cpn10-*del*25) and human mitochondria (*hm*cpn10). We find that the midpoints for the heptamer-monomer equilibrium occur at 0.51 $\pm$ 0.03 μM and 3.5 $\pm$ 0.1 μM total monomer concentration (25°C), for *Aa*cpn10-*del*25 and *hm*cpn10, respectively. For both proteins, association involves endothermic enthalpy and positive entropy changes; thus, the reactions are driven by the entropy increase. This is in accord with the release of ordered water molecules and, for the thermophilic variant, a relaxation of monomer-tertiary structure when the heptamers form.

INTRODUCTION

Complexes resulting from noncovalent protein-protein recognition play a fundamental role in most biological functions. In addition to heterogeneous protein-protein complexes, many proteins are oligomeric due to the association of identical subunits (1). Isothermal titration calorimetry (ITC) is a powerful technique to study interactions between two different proteins and between proteins and their ligands in vitro (2,3). It is the only method that directly determines all the thermodynamic parameters of a given reaction, by measuring the reaction heat as a function of concentration. The self-association of a protein leading to the formation of homo-oligomers has usually not been studied by ITC since it is impossible to isolate individual partners and perform a standard mixing assay. However, it has been reported that the strength of homo-dimer interactions, such as in the interleukin-8 and bovine insulin systems, can be measured in ITC-dilution experiments (3–5). If an oligomeric protein in the syringe is added stepwise to a cell containing only buffer, the dilution will, if the concentration is appropriate, result in oligomer dissociation in the cell. We demonstrate here the applicability of this approach to the study of two co-chaperonin proteins 10 (cpn10) that are homo-heptamers.

The primary function of cpn10 is to assist cpn60 in folding of nonnative proteins. Upon binding to cpn60, the heptameric donutlike ring of cpn10 forms a cap covering the central cavity of cpn60, and the folding of substrates is achieved through cycles of ATP-dependent binding and dissociation (6–9). The tertiary and quaternary structures of cpn10 appear conserved throughout Nature. Cpn10 from *Escherichia coli*, GroES, is the most thoroughly studied co-chaperonin protein and a crystal structure has been described (10). Each GroES subunit adopts an irregular β-barrel topology. The dominant interaction between the subunits in the heptamer ring is an antiparallel pairing of the first β-strand in one subunit and the final β-strand in the next subunit (10). The residues at the interface are highly conserved and have mostly hydrophobic side chains. Human mitochondrial cpn10 (*hm*cpn10) is 37% identical to GroES in terms of primary structure. X-ray and NMR studies have demonstrated that *hm*cpn10 has an identical structure (and thus similar interfaces) to that of GroES (11).

The midpoints for heptamer-monomer dissociation occur at 0.7 μM and 3 μM total monomer concentration, for GroES (12) and *hm*cpn10 (13), respectively, as determined by analytical ultracentrifugation and fluorescence changes, respectively. If folding and assembly processes are coupled (i.e., if isolated monomers are not folded), this modest protein-protein affinity may be explained by a significant loss of entropy upon oligomerization. However, in disagreement, monomeric *hm*cpn10 adopts a folded structure in solution at conditions below the K_D (14) and GroES populates a monomeric intermediate that is at least partially folded during chemically induced equilibrium unfolding (15). To obtain mechanistic insight into the assembly process, we have probed the entropic and enthalpic contributions to the Gibbs-free energy of association via ITC for cpn10 proteins from two different species: *hm*cpn10 and cpn10 from the hyperthermostable bacterium *Aquifex aeolicus* (Fig. 2, *insets*). *A. aeolicus* cpn10 contains a C-terminal 25-residue extension not found in any other cpn10 sequence. This peptide extension is situated after the conserved C-terminal β-strand

Submitted May 23, 2005, and accepted for publication August 1, 2005.

Address reprint requests to P. Wittung-Stafshede, Dept. of Biochemistry and Cell Biology, MS-140, Rice University, 6100 Main St., Houston, TX 77251. Tel.: 713-348-4076; E-mail: pernilla@rice.edu.

0006-3495/05/11/3332/05 $2.00

doi: 10.1529/biophysj.105.067223

that is part of the monomer-monomer interface. To be able to make direct comparisons with other cpn10 proteins, we prepared a truncated version of *A. aeolicus* cpn10 that lacks the last 25 residues (*Aa*cpn10-*del*25). *Aa*cpn10-*del*25 shares 45% and 38% sequence identity with GroES and *hm*cpn10 sequences, respectively. Biophysical work on *Aa*cpn10 (full-length) and *Aa*cpn10-*del*25 have shown that both proteins are heptameric and exhibit similar activity to GroES and *hm*cpn10 in a GroEL-dependent refolding assay (16). Our ITC-dilution experiments demonstrate that the assembly processes of both *hm*cpn10 and *Aa*cpn10-*del*25 heptamers are entropy-driven. This is explained by a release of ordered water molecules from the hydrophobic interfaces upon association.

MATERIALS AND METHODS

Preparation of *hm*cpn10 and *Aa*cpn10

Purification of recombinant *hm*cpn10 expressed in *E. coli* has been described (11,17). Purification of cpn10 from *A. aeolicus* expressed in *E. coli* has also been reported (16). Since the latter protein has a C-terminal extension not found in any other cpn10 protein (16), we created a deletion variant lacking the last 25 residues at the C-terminus (here abbreviated as *Aa*cpn10-*del*25). *Aa*cpn10-*del*25 retains wild-type-like secondary, tertiary, and quaternary structure, as well as thermal stability, as determined by a range of biophysical experiments (K.L. and P.W.-S., unpublished results). Homology modeling (SWISS-MODEL (18,19)) using *Aa*cpn10-*del*25's primary structure predicts a heptamer structure identical to that of GroES with an RMS deviation of the C_αs of 1.6 Å and to that of *Thermus thermophilus* cpn10 with an RMS deviation of the C_αs of 0.3 Å. Protein concentrations were determined from $\varepsilon_{280} = 4200\ M^{-1}\ cm^{-1}$ (*hm*cpn10) and $\varepsilon_{280} = 4460\ M^{-1}\ cm^{-1}$ (*Aa*cpn10-*del*25). All protein concentrations reported herein are per monomer.

Isothermal titration calorimetry (ITC)

Measurements of heat changes linked to heptamer-monomer dissociation were made in a VP-ITC (MicroCal, Northhampton, MA) at 25°C. The *hm*cpn10 samples were dialyzed against 5 mM phosphate buffer, pH 7; the *Aa*cpn10-*del*25 samples were dialyzed against 25 mM Tris-HCl, pH 7.5. All samples were filtered through a 0.22-μm sterile filter membrane (Millipore, Billerica, MA), and degassed at 25°C (ThermoVac, MicroCal) before loading into the ITC syringe. Injection schedules that were found to cover appropriate protein-concentration ranges in the cell (1.4 ml volume) were 3-μl additions of 25 μM *hm*cpn10 and 3-μl additions of 5 μM *Aa*cpn10-*del*25, all spaced between 5-min intervals. The background heats from dilution of the proteins were estimated from the constant heats produced by the injections at very high protein concentrations (i.e., in the latter part of the titrations; here, the fraction heptamer in the syringe and in the cell is roughly similar and close to 1). In each case, this value was subtracted out before data analysis. For all conditions studied, at least two independent experiments were performed. The resulting isotherms were analyzed as described in the text.

RESULTS

The closest relatives to *Aa*cpn10-*del*25 in terms of primary structure are *Thermus thermophilus* cpn10 and GroES (16,20,21). Therefore, the initial ITC-dilution experiments were designed based on the reported heptamer-monomer midpoints for *hm*cpn10 and GroES (no biophysical studies have been reported for *T. thermophilus* cpn10). With appropriate protein concentration (assuring mostly heptamers) in the syringe, the first set of injections into the cell will result in complete dissociation and thus give the largest heat-changes. The injections that follow will reveal a gradual decrease in the heat-changes as the protein concentration in the cell approaches the concentration of the heptamer-monomer midpoint. Finally, when the concentration in the cell reaches well above the heptamer-monomer midpoint concentration (i.e., toward the end of the titration), injections will not result in dissociation and there will only be heat-changes associated with sample dilution. In Fig. 1, we show a representative figure of thermal power as a function of time for a cpn10-dilution experiment. In Fig. 2, we show the corresponding integrated heat changes as a function of total monomer concentration in the cell for ITC-dilution experiments with *Aa*cpn10-*del*25 (Fig. 2 *A*) and *hm*cpn10 (Fig. 2 *B*). It is immediately clear that in both cases, heptamer dissociation corresponds to negative enthalpy which, therefore, means that association is an endothermic process.

The data in Fig. 2, *A* and *B*, reports on the individual heat change associated with each separate injection $q_{obs}(i)$ and, therefore, the midpoints of the transitions do not correspond to the midpoints of the heptamer-monomer dissociation equilibria. The data was analyzed via an iterative nonlinear least-square algorithm to obtain K_D (i.e., the heptamer-monomer dissociation constant) and ΔH_D (i.e., the heptamer-monomer dissociation enthalpy; in per monomer units) values for the heptamer-monomer dissociation reactions as described below.

The relation between Y (fraction monomer) and $[M]_{tot}$ (total monomer concentration) for a heptamer-monomer equilibrium is a seventh-order polynomial:

$$Y^7 + (Y \times K_D)/(7 \times [M]_{tot}^6) - (K_D)/(7 \times [M]_{tot}^6) = 0. \quad (1)$$

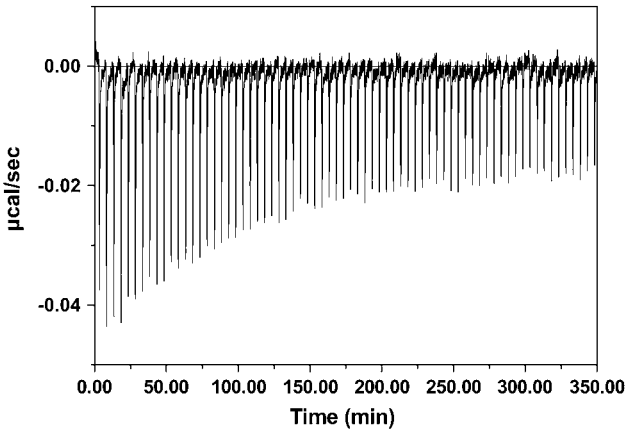

FIGURE 1 The figure shows a representative thermogram of thermal power (μcal/s) as a function of time (min) for an ITC-dilution experiment with one of the cpn10 proteins (*Aa*cpn10-*del*25 data shown).

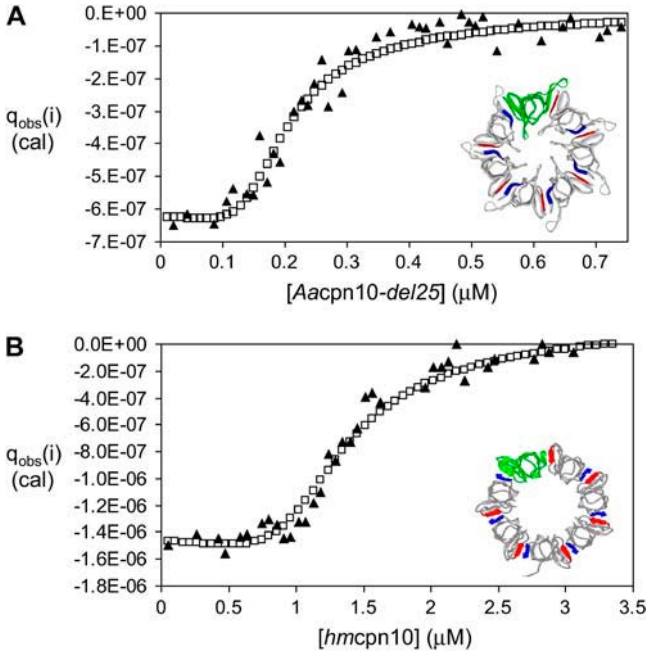

FIGURE 2 Heat changes ($q_{obs}(i)$) versus total monomer concentration ($[M]_{tot,i}$) in the cell for (*A*) *Aa*cpn10-*del*25 and (*B*) *hm*cpn10. Squares are calculated heat changes using optimized values of K_D and ΔH_D (Table 1; nonlinear-regression procedure described in text). (*Insets*) Cartoon illustrations of (in *A*) the *Aa*cpn10-*del*25 structural model and (in *B*) the crystal structure of *hm*cpn10; in both heptamers, one monomer is shown in green and all interface-forming β-strands are shown in blue and red (the *hm*cpn10 structure does not include resolved loops).

Although there appears to be no analytical solutions to Eq. 1, it can be solved numerically. Using an assigned value of K_D and the protein concentration in the syringe ($[M]_{tot,syr}$), Eq. 1 was first solved to obtain the fraction of monomer in the syringe (Y_{syr}). Next, accounting for the protein-concentration in the syringe, the cell volume and the injection volume, the total concentration of protein in the cell after each injection i was calculated ($[M]_{tot,i}$). Then, the fraction of monomers (Y_i) and heptamers in the cell was calculated after each injection i by solving Eq. 1. We note that not all monomers in the cell come from heptamer dissociation upon injection since there is a fraction of monomers in the syringe and, therefore, monomers are also injected from the syringe. From the increment in monomer concentration in the cell after each injection, also accounting for the fraction of monomers coming directly from the syringe, the heat associated with each injection (i.e., $q_{obs}(i)$) was calculated according to Eq. 2 and an assigned value of ΔH_D (3,4):

$$q_{obs}(i) = \Delta H_D \times [Y_i \times n(i) - Y_{i-1} \times n(i-1) - Y_{syr} \times n(inj)]. \quad (2)$$

Here, Y_i is the fraction monomer in the cell after injection i, and Y_{i-1} is the fraction monomer in the cell after the previous, $i-1$, injection. Furthermore, $n(i)$ is the number of moles of total monomer in the reaction cell after injection i ($= V \times [M]_{tot,i}$; where V is the reaction-cell volume), and $n(i-1)$ is the number of moles of total monomer in the reaction cell after injection $i-1$ ($= V \times [M]_{tot,i-1}$). Y_{syr} is the fraction monomers in the injected sample, i.e., the fraction monomer in the syringe, and $n(inj)$ is the number of moles of total monomers injected into the reaction cell at each injection ($= v \times [M]_{tot,syr}$; where v is the injected volume).

The calculated heats were compared with the experimental ones and the complete procedure was repeated (with slightly modified K_D and ΔH_D values each time) until convergence was achieved and the experimental $q_{obs}(i)$ versus $[M]_{tot}$ data could be accurately reproduced (Fig. 2). The optimized K_D (corresponding to midpoints at 3.5- and 0.51-μM total monomer concentration for *hm*cpn10 and *Aa*cpn10-*del*25, respectively) and ΔH_D (-23.5 and -44.5 kcal/mol for *hm*cpn10 and *Aa*cpn10-*del*25, respectively) values for both proteins are reported in Table 1. K_D is related to the Gibbs-free energy of dissociation via $\Delta G_D = -RT\ln K_D$ and ΔS_D is calculated from $\Delta G_D = \Delta H_D - T\Delta S_D$. All thermodynamic parameters calculated for assembly of the two cpn10 heptamers are summarized in Table 1.

DISCUSSION

The excellent agreement between heptamer-monomer concentration midpoints identified via ITC and by earlier biophysical methods gives the ITC-dilution method validity. We report an ITC-derived midpoint for *hm*cpn10 of 3.5 μM and earlier fluorescence studies revealed a midpoint of $\sim$3 μM at similar conditions (pH 7, phosphate buffer, 20°C) (13). For GroES, a midpoint of 0.7 μM was reported from analytical-ultracentrifugation experiments at 20°C (12); we find a midpoint of 0.51 μM by ITC for the homologous *Aa*cpn10-*del*25 heptamer (Table 1). No experimental information on the enthalpic and entropic contributions to cpn10 heptamer formation has been reported. It was proposed that, from structure-based thermodynamic calculations on the GroES crystal structure, heptamer association should be favorable both enthalpically and entropically (22). However, this calculation assumed that folding of isolated monomers was very unfavorable. Although isolated monomers have

TABLE 1 Thermodynamic parameters for the heptamer-monomer equilibria for *Aa*cpn10-*del*25 and *hm*cpn10 calculated from the ITC-dilution experiments as described in the text

Protein	Midpoint (μM)	ΔG_A (kJ/mol)	ΔH_A (kJ/mol)	ΔS_A (J/mol,K)
*Aa*cpn10-*del*25	0.51 ($\pm$0.03)	-31.5 ($\pm$0.5)	+186 ($\pm$8)	+730 ($\pm$30)
*hm*cpn10	3.5 ($\pm$0.1)	-27.4 ($\pm$0.5)	+98 ($\pm$4)	+420 ($\pm$20)
*hm*cpn10	3*	-27.8	–	–
GroES	0.7†	-31	–	–

For comparison, available data for GroES is also shown. All values correspond to assembly (indicated by subscript *A*) at 25°C, pH 7 (*hm*cpn10) or 7.5 (*Aa*cpn10-*del*25), and are given per mol monomer.
*From dilution experiments measuring fluorescence changes (13).
†From analytical ultracentrifugation experiments (12).

low thermodynamic stability, it is clear from recent work that they adopt folded structures in solution (14).

Our ITC experiments directly demonstrate that assembly of *hm*cpn10 and *Aa*cpn10-*del*25 is accompanied by unfavorable (i.e., endothermic) enthalpy (98 and 186 kJ/mol, respectively) and favorable (i.e., positive) entropy (420 and 730 J/mol,K, respectively). The overall enthalpy change may include three major terms: 1), conformational enthalpy; 2), interaction enthalpy; and 3), solvation enthalpy (23). Conformational enthalpy is generally exothermic since formation of secondary structure is favorable; however, since the cpn10 monomers are probably folded in solution (14), this term will be negligible. The second term is also exothermic, since it involves the formation of new noncovalent interactions such as electrostatic attraction, van der Waals interactions, and hydrogen bonds (23). Since the overall enthalpy change is endothermic in the case of cpn10, the second term is likely compensated for by a large positive third term, which involves the release of ordered water molecules from the monomer surfaces that form the interfaces. This reaction is enthalpically unfavorable since it involves the breakage of hydrogen and ionic bonds. The positive entropy associated with cpn10 assembly follows the classical hydrophobic effect, which is an entropy-driven process. Partitioning of a nonpolar molecule from water to a nonpolar phase is accompanied by an increase in the entropy of the system (24). Since the cpn10 interfaces are mostly hydrophobic (10,11), there may be a significant number of ordered waters released upon assembly. Thus, both the favorable entropy and the unfavorable enthalpy can be explained by a release of ordered water molecules upon heptamer assembly.

An alternative source for endothermic enthalpy and positive entropy accompanying association is the idea of structural loosening of the monomer structure (25). This phenomenon has been shown to correspond to endothermic enthalpies and positive entropies and several biological examples have been reported (e.g., peptide-membrane interactions (25) and complex formation between metalloprotease inhibitor N-TIMP-1 and stromelysin 1 (26)). The crystal structure of GroES shows that the interfaces may have high plasticity since there are clear deviations in side-chain and backbone positions when comparing the seven interfaces (10). Thus, the cpn10 monomers may adopt compact structures in solution to avoid exposing too much hydrophobic surface to the solvent. These compact structures then need to relax (loosen up) in order to form the interfaces in the heptameric structure.

Structure-based thermodynamic parameterization of the assembly reaction for GroES has been reported (22). The GroES crystal structure was used for this and the calculations, defined in (27–31), decomposed the Gibbs free energy into generic, ionic, and translational components. The calculated entropy of (de)solvation, based on the surface area buried upon assembly, was reported to be +390 J/mol,K for GroES at 25°C (per monomer) (22). If we assume that both *hm*cpn10 and *Aa*cpn10-*del*25 bury similar surfaces in terms of both side chains and areas upon assembly, which is reasonable due to the high structural and sequence homology to GroES, this implies that desolvation (i.e., water release) accounts for most of the positive entropy involved in *hm*cpn10 assembly (+420 J/mol,K; Table 1). However, *Aa*cpn10-*del*25 assembly involves significantly larger values of both the endothermic enthalpy and the positive entropy than *hm*cpn10 assembly (Table 1). Therefore, in the case of *Aa*cpn10-*del*25, approximately half of the total entropy gain upon assembly may be due to structural loosening [730 J/mol,K (total) − 390 J/mol,K (solvation) = 340 J/mol,K (structural loosening)]. This difference between *hm*cpn10 and *Aa*cpn10-*del*25 can be explained by the thermophilic origin of *A. aeolicus* resulting in the *Aa*cpn10-*del*25 monomers being more rigid than *hm*cpn10 monomers at 25°C. In support, preliminary work demonstrates that *Aa*cpn10-*del*25 monomers are greater than twice as stable toward chemical denaturation as are the *hm*cpn10 monomers (K.L. and P.W.-S., unpublished results). The structure-based estimate for the conformational entropy corresponding to complete unfolding of the GroES monomer is ~1600 J/mol,K (22). Since this value is much higher than the entropy assigned to structural loosening of *Aa*cpn10-*del*25 (~340 J/mol,K, see above), it appears that the relaxation only involves ~20% of the *Aa*cpn10-*del*25 structure.

We note that the *hm*cpn10 and *Aa*cpn10-*del*25 experiments were performed in different buffers. In part, this was a strategic choice to allow for comparisons of dissociation midpoints with earlier studies. In addition, *Aa*cpn10-*del*25 precipitates in phosphate buffer and *hm*cpn10 has been reported to exist as a mixture of various oligomeric species in Tris-HCl buffer (32), which we also confirmed by glutaraldehyde crosslinking experiments, precluding comparisons in the same buffer. Phosphate and Tris-HCl buffers have different ionization energies (~2 kcal/mol and ~11 kcal/mol, respectively (27)) and, therefore, protonation/deprotonation events (if they occur) will give different contributions to the enthalpy change of heptamer assembly in the two buffers. We will address the involvement of protonation/deprotonation in the heptamer-assembly processes of the two proteins in a future study involving ITC experiments in a range of buffers with different ionization energies and in which the cpn10 proteins are soluble and heptameric.

In summary, we here demonstrate that ITC is a useful method for thermodynamic analysis of heptameric homo-oligomeric systems. Moreover, we establish that cpn10 assembly is an endothermic reaction that is entropy-driven. This is explained by the release of ordered water from hydrophobic surfaces (both *Aa*cpn10-*del*25 and *hm*cpn10) and structural loosening of the monomers (only *Aa*cpn10-*del*25) upon heptamer formation.

We thank C. Brown for preparing *hm*cpn10.

Support for this project was provided by grants from the National Institutes of Health (No. GM059663) and the Robert A. Welch Foundation (No. C-1588). K.L. is supported by a fellowship from a National Institutes of Health Biotechnology Research Training Grant.

REFERENCES

1. Traut, T. W. 1994. Dissociation of enzyme oligomers: a mechanism for allosteric regulation. *Crit. Rev. Biochem. Mol. Biol.* 29:125–163.
2. Wiseman, T., S. Williston, J. F. Brandts, and L. N. Lin. 1989. Rapid measurement of binding constants and heats of binding using a new titration calorimeter. *Anal. Biochem.* 179:131–137.
3. Velazquez-Campoy, A., S. A. Leavitt, and E. Freire. 2004. Characterization of protein-protein interactions by isothermal titration calorimetry. *Methods Mol. Biol.* 261:35–54.
4. Burrows, S. D., M. L. Doyle, K. P. Murphy, S. G. Franklin, J. R. White, I. Brooks, D. E. McNulty, M. O. Scott, J. R. Knutson, D. Porter, P. R. Young, and P. Hensley. 1994. Determination of the monomer-dimer equilibrium of interleukin-8 reveals it is a monomer at physiological concentrations. *Biochemistry.* 33:12741–12745.
5. Lovatt, M., A. Cooper, and P. Camilleri. 1996. Energetics of cyclodextrin-induced dissociation of insulin. *Eur. Biophys. J.* 24:354–357.
6. Martin, J., S. Geromanos, P. Tempst, and F. U. Hartl. 1993. Identification of nucleotide-binding regions in the chaperonin proteins GroEL and GroES. *Nature.* 366:279–282.
7. Todd, M. J., O. Boudkin, E. Freire, and G. H. Lorimer. 1995. GroES and the chaperonin-assisted protein folding cycle: GroES has no affinity for nucleotides. *FEBS Lett.* 359:123–125.
8. Burston, S. G., J. S. Weissman, G. W. Farr, W. A. Fenton, and A. L. Horwich. 1996. Release of both native and non-native proteins from a *cis*-only GroEL ternary complex. *Nature.* 383:96–99.
9. Shtilerman, M., G. H. Lorimer, and S. W. Englander. 1999. Chaperonin function: folding by forced unfolding. *Science.* 284:822–825.
10. Hunt, J. F., A. J. Weaver, S. J. Landry, L. Gierasch, and J. Deisenhofer. 1996. The crystal structure of the GroES co-chaperonin at 2.8 Å resolution. *Nature.* 379:37–45.
11. Landry, S. J., N. K. Steede, and K. Maskos. 1997. Temperature dependence of backbone dynamics in loops of human mitochondrial heat shock protein 10. *Biochemistry.* 36:10975–10986.
12. Zondlo, J., K. E. Fisher, Z. Lin, K. R. Ducote, and E. Eisenstein. 1995. Monomer-heptamer equilibrium of the *Escherichia coli* chaperonin GroES. *Biochemistry.* 34:10334–10339.
13. Guidry, J. J., C. K. Moczygemba, N. K. Steede, S. J. Landry, and P. Wittung-Stafshede. 2000. Reversible denaturation of oligomeric human chaperonin 10: denatured state depends on chemical denaturant. *Protein Sci.* 9:2109–2117.
14. Guidry, J. J., and P. Wittung-Stafshede. 2002. Low stability for monomeric human chaperonin protein 10: interprotein interactions contribute majority of oligomer stability. *Arch. Biochem. Biophys.* 405:280–282.
15. Higurashi, T., K. Nosaka, T. Mizobata, J. Nagai, and Y. Kawata. 1999. Unfolding and refolding of *Escherichia coli* chaperonin GroES is expressed by a three-state model. *J. Mol. Biol.* 291:703–713.
16. Guidry, J., and P. Wittung-Stafshede. 2004. First characterization of co-chaperonin protein 10 from hyper-thermophilic *Aquifex aeolicus*. *Biochem. Biophys. Res. Commun.* 317:176–180.
17. Steede, N. K., J. J. Guidry, and S. J. Landry. 2000. Preparation of recombinant human Hsp10. *Methods Mol. Biol.* 140:145–151.
18. Guex, N., and M. C. Peitsch. 1997. SWISS-MODEL and the Swiss-PdbViewer: an environment for comparative protein modeling. *Electrophoresis.* 18:2714–2723.
19. Schwede, T., J. Kopp, N. Guex, and M. C. Peitsch. 2003. SWISS-MODEL: an automated protein homology-modeling server. *Nucleic Acids Res.* 31:3381–3385.
20. Numoto, N., A. Kita, and K. Miki. 2005. Crystal structure of the co-chaperonin Cpn10 from *Thermus thermophilus* HB8. *Proteins.* 58: 498–500.
21. Shimamura, T., A. Koike-Takeshita, K. Yokoyama, R. Masui, N. Murai, M. Yoshida, H. Taguchi, and S. Iwata. 2004. Crystal structure of the native chaperonin complex from *Thermus thermophilus* revealed unexpected asymmetry at the *cis*-cavity. *Structure (Cambridge.).* 12:1471–1480.
22. Boudker, O., M. J. Todd, and E. Freire. 1997. The structural stability of the co-chaperonin GroES. *J. Mol. Biol.* 272:770–779.
23. Abraham, T., R. N. Lewis, R. S. Hodges, and R. N. McElhaney. 2005. Isothermal titration calorimetry studies of the binding of a rationally designed analogue of the antimicrobial peptide gramicidin S to phospholipid bilayer membranes. *Biochemistry.* 44:2103–2112.
24. Tanford, C. 1978. The hydrophobic effect and the organization of living matter. *Science.* 200:1012–1018.
25. Williams, D. H., D. P. O′Brien, A. M. Sandercock, and E. Stephens. 2004. Order changes within receptor systems upon ligand binding: receptor tightening/oligomerisation and the interpretation of binding parameters. *J. Mol. Biol.* 340:373–383.
26. Sengchanthalangsy, L. L., S. Datta, D. B. Huang, E. Anderson, E. H. Braswell, and G. Ghosh. 1999. Characterization of the dimer interface of transcription factor NFκB p50 homodimer. *J. Mol. Biol.* 289:1029–1040.
27. Gomez, J., and E. Freire. 1995. Thermodynamic mapping of the inhibitor site of the aspartic protease endothiapepsin. *J. Mol. Biol.* 252:337–350.
28. Gomez, J., V. J. Hilser, D. Xie, and E. Freire. 1995. The heat capacity of proteins. *Proteins.* 22:404–412.
29. Hilser, V. J., and E. Freire. 1996. Structure-based calculation of the equilibrium folding pathway of proteins. Correlation with hydrogen exchange protection factors. *J. Mol. Biol.* 262:756–772.
30. Hilser, V. J., J. Gomez, and E. Freire. 1996. The enthalpy change in protein folding and binding: refinement of parameters for structure-based calculations. *Proteins.* 26:123–133.
31. Bardi, J. S., I. Luque, and E. Freire. 1997. Structure-based thermodynamic analysis of HIV-1 protease inhibitors. *Biochemistry.* 36: 6588–6596.
32. Fossati, G., P. Lucietto, P. Giuliani, A. R. Coates, S. Harding, H. Colfen, G. Legname, E. Chan, A. Zaliani, and P. Mascagni. 1995. *Mycobacterium tuberculosis* chaperonin 10 forms stable tetrameric and heptameric structures. Implications for its diverse biological activities. *J. Biol. Chem.* 270:26159–26167.